IEEE Access
Multidisciplinary | Rapid Review | Open Access Journal

Received 13 December 2024, accepted 6 January 2025, date of publication 8 January 2025, date of current version 15 January 2025.

Digital Object Identifier 10.1109/ACCESS.2025.3527057

RESEARCH ARTICLE

Telecommand Rejection Probability in CCSDS-Compliant LDPC-Coded Space Transmissions With Tail Sequence

REBECCA GIULIANI[1,2], (Graduate Student Member, IEEE), MASSIMO BATTAGLIONI[1,2], (Member, IEEE), MARCO BALDI[1,2], (Senior Member, IEEE), FRANCO CHIARALUCE[1,2], (Senior Member, IEEE), AND NICOLA MATURO[3], (Member, IEEE)

[1]Department of Information Engineering, Università Politecnica delle Marche, 60131 Ancona, Italy
[2]Consorzio Nazionale Interuniversitario per le Telecomunicazioni (CNIT), 43124 Parma, Italy
[3]European Space Agency, ESTEC, 2200 AG Noordwijk, The Netherlands

Corresponding author: Rebecca Giuliani (r.giuliani@pm.univpm.it)

This work was [supported/partially supported] by the European Union - Next Generation EU under the Italian National Recovery and Resilience Plan (NRRP), Mission 4, Component 2, Investment 1.3, CUP J33C22002880001, partnership on "Telecommunications of the Future" (PE00000001 - program "RESTART").

ABSTRACT According to the Consultative Committee for Space Data Systems (CCSDS) recommendation for Telecommand (TC) synchronization and coding, the Communications Link Transmission Unit (CLTU) consists of a start sequence, followed by coded data, and a tail sequence, which might be optional depending on the employed coding scheme. With regard to the latter, these transmissions traditionally use a modified Bose–Chaudhuri–Hocquenghem (BCH) code, to which two state-of-the-art Low-Density Parity-Check (LDPC) codes were later added. A low-complexity approach classically used to detect CLTU termination is to choose a non-correctable string as the tail sequence, and then exploit the decoder failure on that sequence as termination detection. This works very well with the BCH code, for which bounded-distance decoders are employed. Instead, when the same approach is employed with LDPC codes and probabilistic belief propagation iterative decoders, the scenario becomes more challenging. In this paper, we study CCSDS-compliant space communications in which LDPC codes are employed, and analyze the TC rejection probability both theoretically and through intensive numerical simulations. Such a performance figure, being the rate at which CLTUs are discarded, should clearly be minimized. Our numerical analysis considers many different choices of the system parameters (e.g., length of the CLTU, decoding algorithm, maximum number of decoding iterations). Particular attention is devoted to the probability of not-acknowledged termination, i.e., the probability that the tail sequence is not recognized.

INDEX TERMS LDPC codes, satellite communications, tail sequence, Telecommand.

I. INTRODUCTION

In space missions, the TeleCommand (TC) function plays a crucial role, in that it is responsible for the transmission of commands to the spacecraft. The Consultative Committee for Space Data Systems (CCSDS) suggests that, in order to be reliably received and correctly processed by the space element, raw data need to be encoded and encapsulated into a Communications Link Transmission Unit (CLTU). According to [1], and as described in [2], the CLTU should be formed, sequentially, by:

- a start sequence, aimed at synchronizing the beginning of a CLTU and at delimiting the beginning of the first codeword;
- a certain number of codewords, say N, representing the encoded data;
- a Tail Sequence (TS), delimiting the end of the CLTU, that is optional, depending on the employed error correcting coding scheme.

The associate editor coordinating the review of this manuscript and approving it for publication was Zilong Liu.

The structure of the CLTU is shown in Fig. 1. Due to its role, the start sequence should be designed as a pattern with good autocorrelation properties, such that the use of a classical correlation-based detector yields negligible probability of confusing it with another pattern. When transmission over an Additive White Gaussian Noise (AWGN) channel is considered, the optimal strategy to detect noisy versions of a periodically inserted sync sequence is through the algorithm proposed in [3]. If there is a single sync sequence, it is possible to use the Simplified Likelihood Ratio Test (S-LRT) [4], [5].

As for data reliability, many error correcting coding schemes might be adopted to mitigate the effect of the noise introduced by the channel. Notable examples are Bose–Chaudhuri–Hocquenghem (BCH) codes and Low-Density Parity-Check (LDPC) codes, first introduced in the seminal works [6], [7] and [8], respectively. These families of codes are those recommended by the CCSDS in [1].

Differently from the start sequence, the design of the Tail Sequence (TS) is quite challenging, because it must take into account the technique used for its detection. Despite this, TS design has received little attention in the scientific literature. Possible methods include using a hard/soft correlator, or the S-LRT [4], similar to the approach for the start sequence. An engaging alternative is that of designing the TS in such a way that it triggers an error in the decoding process [9]. This way, the receiver does not need to switch between devices (decoder and correlator), and just continues decoding until it fails. It is important to note that each method imposes distinct requirements. For example, the former approaches generally require low side lobes in the auto-correlation function, while the latter technique demands that the TS provides an "uncorrectable" error pattern, ensuring (with high enough probability) that the decoder does not misinterpret it as a codeword. Fortunately, these requirements are not mutually exclusive.

A. OUR CONTRIBUTION

In this paper, we study and assess the performance of a communication system that incorporates error-correcting codes and a TS. We assess the TC rejection probability both theoretically, where feasible, and numerically using Monte Carlo simulations, otherwise. This metric is crucial for evaluating the system performance as it determines the rate at which CLTUs are discarded and, consequently, the TC cannot be used by the space element.

In particular, we focus on the CCSDS-compliant scenario in which:

- data are encoded with an LDPC error-correcting code, and consequently decoded by iterative algorithms;
- the TS is detected by exploiting the trigger of a decoding error.

To the best of our knowledge, a thorough study of the performance of LDPC-coded transmissions provided with a termination pattern detected through decoding failures is missing in the literature, and this motivates our work.

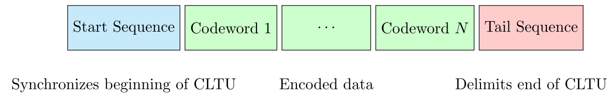

FIGURE 1. CLTU structure [1].

As for LDPC decoding algorithms, we consider the Log-Likelihood Ratio Sum-Product Algorithm (LLR-SPA) [10], the Min-Sum Algorithm (MSA) [11], and the Normalized Min-Sum Algorithm (NMSA) [12]. We study the system performance by considering several values of the maximum number of decoding iterations and CLTU lengths, showing that, somehow counterintuitively, a small number of decoding iterations can improve performance, from the TS detection standpoint, when the CLTU is extremely short.

Our study starts from [1] but considers a more general framework. Moreover, when using the parameters recommended in [1], our numerical results indicate that the performance of the current system falls short of expectations, seriously mining the reliability of the current standard. To explain this finding, we develop an in-depth analysis of decoding in the setting under exam. Following such an analysis, we suggest a modification to the standard system aimed at reducing the TC rejection probability. Throughout the paper, we provide some theoretical insights to understand and justify the results obtained.

B. PAPER OUTLINE

The paper is organized as follows. In Section II we establish the necessary context. In Section III we analyze the TC rejection probability, and provide insights on the single contributions forming it. In Section IV we assess the whole system performance in the standard case. In Section V we propose a solution to improve it, and provide numerical results to justify the improvement. Section VI is devoted to practical scenarios where the CLTU contains more than one codeword. Finally, Section VII provides some concluding remarks.

II. PRELIMINARIES

In this section, we introduce the terminology and notation used throughout the paper, and provide a brief overview of the communication system established in [1].

A. NOTATION

The Hamming distance between two vectors with n components, $\mathbf{a} = [a_0, a_1, \ldots, a_{n-1}]$ and $\mathbf{b} = [b_0, b_1, \ldots, b_{n-1}]$, is defined as the number of positions at which they differ, and is denoted as $d_{\mathrm{H}}(\cdot)$. Instead, the Euclidean distance is denoted as $d_{\mathrm{E}}(\cdot)$ and is defined as follows:

$$d_{\mathrm{E}}(\mathbf{a}, \mathbf{b}) = \sqrt{(a_0 - b_0)^2 + \ldots + (a_{n-1} - b_{n-1})^2}.$$

The Hamming weight of a vector is given by the number of its non-zero entries.

Given the finite field $\mathbb{F}_2$, an (n, k) linear binary code $\mathcal{C}$ is a k-dimensional subspace of $\mathbb{F}_2^n$, where $k < n$. The codewords in $\mathcal{C}$ can be obtained as $\mathcal{C} = \{\mathbf{c} \in \mathbb{F}_2^n | \mathbf{c}\mathbf{H}^\top = \mathbf{0}\}$, where $\top$ denotes transposition, and $\mathbf{H} \in \mathbb{F}_2^{r \times n}$ is a full-rank matrix of size $r \times n$, where $r = n - k$, which is known as the parity-check matrix. The code rate R is defined as $R = \frac{k}{n}$. The number of codewords of Hamming weight w is denoted as $A(w)$, often referred to as weight enumerator function or distance distribution. Since the considered error correcting codes are linear, the minimum Hamming distance of the code, simply denoted as $d_{\min}$, is the smallest positive value of w in the code such that $A(w) > 0$. In a linear code, all codewords have identical Hamming distance properties; therefore, $A(w)$ also represents the number of codewords at Hamming distance w from any fixed codeword. LDPC codes are characterized by parity-check matrices with a relatively small number of non-zero entries compared to the number of zeros.

B. STANDARD COMMUNICATION SYSTEM

The TC communication system described in [1], for the case using LDPC coding, is summarized in Fig. 2. Basically, the information sequences (infowords) are encoded, then the encoded data are randomized and encapsulated into a CLTU; in this stage, the start sequence and the TS are added, respectively, ahead and behind the encoded data. Two LDPC codes are considered in [1]: a short LDPC code with $n = 128$ and $k = 64$ and a (relatively) long LDPC code with $n = 512$ and $k = 256$. When data are encoded with the $(128, 64)$ LDPC code (described in detail in Appendix A), the inclusion of the TS is optional; instead, for the $(512, 256)$ LDPC code the TS shall not be used at all (see [1, Section 5.2.4.3]). For this reason, we do not discuss further the latter code. The $(128, 64)$ LDPC code code has $R = \frac{1}{2}$ and minimum distance $d_{\min} = 14$ [13]. Note that, if BCH coding is used, a different communication scheme should be employed. In particular, in that case, randomization is optional and, if used, it is applied before the encoding operation.

At the receiver side, the start sequence is detected, then the encoded data and the TS are input to the de-randomizer (therefore, the encoded data are de-randomized, whereas the TS is randomized) and, finally, the decoding process starts. The decoding process stops:

1) if the TS is recognized by a hard/soft correlator (or with any alternative approach specific to the TS detection); or
2) if the decoder reaches a predetermined maximum number of iterations without converging to a codeword.

In this paper, we focus on the latter approach, assuming that the TS is designed as a vector which is sufficiently distant, according to some metric, from the LDPC codewords and thus triggers a decoding failure with high probability.

III. TELECOMMAND REJECTION PROBABILITY

To analyze the system performance, by generalizing [2, Equation (14)], we compute the TC rejection probability, which is the probability that the TC gets rejected from the satellite, when LDPC coding is employed, and the TS ends the CLTU.

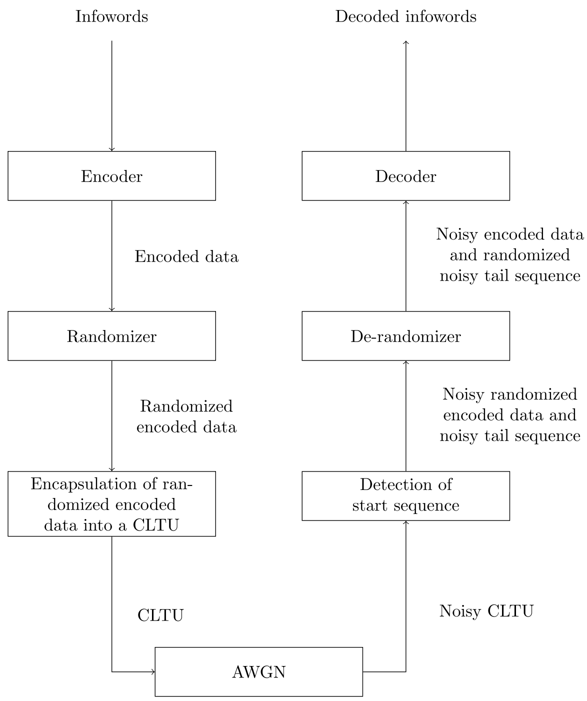

FIGURE 2. Communication system's blocks diagram when using LDPC codes.

The TC rejection probability of the communication system described in Fig. 2 can be computed as

$$P_{\text{TCrej}} = P_{\text{nat}} + (1 - P_{\text{nat}})[P_{\text{md}} + (1 - P_{\text{md}})P_{\text{LDPC}}], \quad (1)$$

where

- P_{md} is the *missed detection probability*, i.e., the probability that the start sequence is not detected;
- P_{nat} is the *not-acknowledged termination probability*, that is, the probability that the termination of the CLTU (that is the TS) is not recognized;
- P_{LDPC} is the probability that decoding fails for any of the LDPC codewords, and the error is detected.

In fact, following the order given in Fig. 1, we readily notice that the TC is rejected if

- the start sequence is not correctly recognized, or if
- the start sequence is correctly detected, but the decoder fails (in a detectable way) to decode any of the N codewords, or if
- the start sequence is correctly detected, and the decoder decodes all the N codewords, but the TS is not recognized.

Since these events are mutually exclusive, the corresponding probabilities can be summed, leading to

$$P_{\text{TCrej}} = P_{\text{md}} + (1 - P_{\text{md}})[P_{\text{LDPC}} + (1 - P_{\text{LDPC}})P_{\text{nat}}].$$

Equation (1) is obtained by solving further the above equation. It is easy to verify that the dominant contribution in (1) is $P_{\text{md}} + P_{\text{nat}} + P_{\text{LDPC}}$, since the other terms are products of two or three probabilities. So, in the following, we will discuss the behavior of these leading components, reasoning on their impact on the overall probability P_{TCrej}.

It is obvious to observe that, when P_{md} and P_{LDPC} tend to 0 (which occurs for high values of the signal-to-noise ratio), P_{TCrej} converges to P_{nat}. This straightforward reasoning will help justifying the performance results, presented in Sections IV and V.

Let us study separately the three leading probabilities contributing to P_{TCrej}, and provide more thorough definitions.

A. MISSED DETECTION PROBABILITY

The missed detection probability P_{md} is the probability that the start sequence is not correctly detected, and therefore the receiver does not recognize the beginning of the CLTU. In order to model P_{md}, we consider that an S-bits start sequence, along with the CLTU, is Binary Phase-Shift Keying (BPSK)-modulated and transmitted over the AWGN channel. Moreover, for the sake of ease, we assume that a bit-by-bit comparison of the (hard) received sequence with the actual start sequence is employed for detection, and that the received sequence is accepted as the start sequence if it differs in up to E positions from the actual start sequence. In other words, the metric we consider is the number of positions in which the tentative sequence and the start sequence match. To be noticed that, if the start sequence is well-designed, this approach corresponds to the use of a hard correlator. The missed detection probability can then be computed, by extending the formulation in [2], as

$$P_{\mathrm{md}} = 1 - \sum_{j=0}^{E} \binom{S}{j} P_b^j (1 - P_b)^{S-j}, \tag{2}$$

where P_b is the bit error probability for BPSK-modulated transmissions over the AWGN channel, that is, $P_b = \frac{1}{2}\mathrm{erfc}\left(\sqrt{\frac{E_b}{N_0}}\right)$, being $\mathrm{erfc}(\cdot)$ the complementary error function and $\frac{E_b}{N_0}$ the signal-to-noise ratio per bit. Equation (2) is obtained by considering that the start sequence is correctly detected if at most E hard errors occurred during transmission.

B. PROBABILITY OF DECODING FAILURE ON CODED DATA

The TC gets rejected also if the decoder fails to converge to a codeword while decoding the LDPC-coded data. Also in this case, we actually need to consider two possible scenarios, corresponding to different decoding errors:

- the decoder does not produce a codeword as output, resulting in a *detectable error*;
- the decoder converges to a codeword that is not the transmitted one, yielding an *undetectable error*.

If an undetectable error occurs, the TC would not be rejected. Therefore, the undetectable error rate should not be considered in the computation of P_{TCrej}.

The overall Codeword Error Rate (CER), that is, the probability that a codeword is incorrectly decoded, can be written as

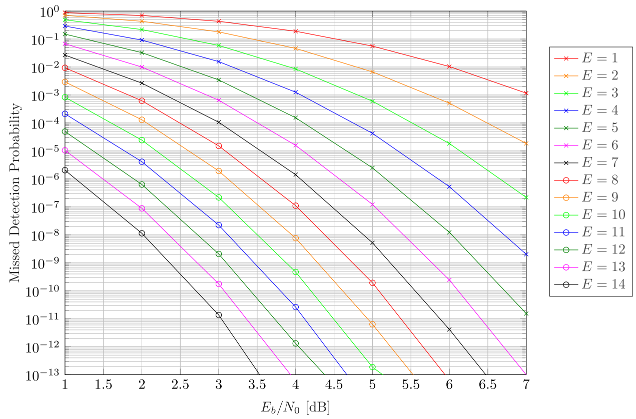

FIGURE 3. Missed detection probability under hard correlation detection, assuming $S = 64$.

$$\mathrm{CER} = \mathrm{CER}^* + \mathrm{UCER},$$

being CER^* the "detectable" CER and UCER the "undetectable" CER. Given this, assuming that the CLTU contains N codewords, based on its definition, we can compute

$$P_{\mathrm{LDPC}} = 1 - (1 - \mathrm{CER}^*)^N. \tag{3}$$

For practical error-correcting codes and not extremely low values of E_b/N_0 (see, for example, [13, Fig. 11-9]) it is possible to assume

$$\mathrm{CER} \approx \mathrm{CER}^*,$$

since $\mathrm{UCER} \ll \mathrm{CER}^*$ and is thus negligible. The value of the CER will be estimated through Monte Carlo simulations as[1]

$$\mathrm{CER} \approx \frac{\#_{\mathrm{decoding-failures}}}{\#_{\mathrm{decoding-attempts}}}. \tag{4}$$

It is interesting to study the behavior of (3) when N is small to moderate and E_b/N_0 is large. In this setting, it is possible to approximate P_{LDPC} as $1-(1-\mathrm{CER})^N$. In particular, if the CER is small and N is not too large, we can write

$$P_{\mathrm{LDPC}} \approx 1 - (1 - \mathrm{CER})^N \approx N \cdot \mathrm{CER}. \tag{5}$$

C. NOT-ACKNOWLEDGED TERMINATION PROBABILITY

Assuming that the TS is detected by triggering a detectable decoding error, the reasoning on the TC rejection probability is opposite to that of an LDPC decoding failure. In this case, when the noisy (randomized) TS is fed to the decoder, we expect it to fail. If the decoder mistakenly converges to a codeword, it would indicate that it has incorrectly identified the TS as valid encoded data, which is clearly undesirable. We can thus estimate P_{nat} through Monte Carlo simulations, where the TS is the object of the transmission; however, somehow counterintuitively, we have a not-acknowledged termination when the decoder succeeds, whereas the termination is correctly acknowledged if the decoder fails. In other

[1] Here and in the following, # conventionally reads as "Number of".

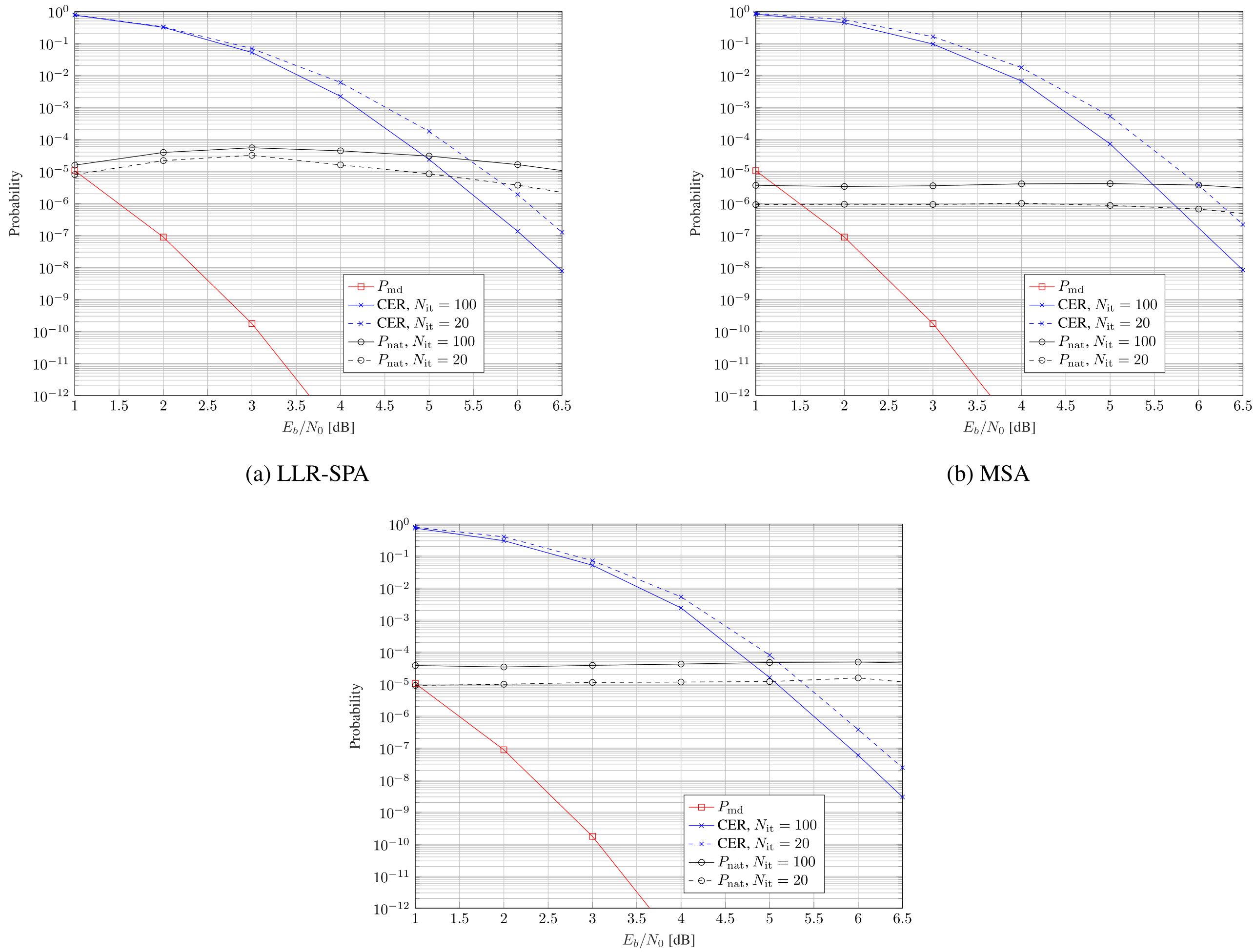

(a) LLR-SPA

(b) MSA

(c) NMSA

FIGURE 4. Comparison of TC rejection probability's leading components for different algorithms (standard case).

words, the Probability of Not-Acknowledged Termination is estimated as

$$P_{\text{nat}} = \frac{\#_{\text{decoding-successes}}}{\#_{\text{decoding-attempts}}} = 1 - \frac{\#_{\text{decoding-failures}}}{\#_{\text{decoding-attempts}}}. \quad (6)$$

We thus notice that the not-acknowledged termination probability is the complementary of the codeword error rate (4), but with different decoder inputs.

In order to minimize the likelihood of a decoding success, the TS can be designed as a pattern that is as far as possible from any codeword of the considered LDPC code, according to the Maximum Likelihood (ML) decoding principle for the AWGN channel. The latter states that, keeping in mind the mapping $\mathbf{x} = (-1)^{\mathbf{c}}$, and receiving $\mathbf{y}$ as input (which is the noisy TS, in our setting), the decoder output is the following estimated codeword $\hat{\mathbf{c}}$:

$$\hat{\mathbf{c}} = \arg\min_{\mathbf{c}} d_{\text{E}}(\mathbf{y}, \mathbf{x}).$$

Clearly, since the TS is a binary vector, a good strategy consists in designing the TS in such a way that its Hamming distance from all the 2^k codewords (the i-th one being denoted as $\mathbf{c}_i$, with $0 \leq i \leq 2^k - 1$) of the (128, 64) LDPC code is the largest possible, i.e., if we denote the TS as $\mathbf{t}$, in such a way that $\min_{0 \leq i \leq 2^k - 1} d_{\text{H}}(\mathbf{t}, \mathbf{c}_i)$ is maximized. It is important to remark that the practical iterative decoders commonly used for decoding LDPC codes are suboptimal compared to ML and, most importantly, they are not complete decoders. As a result, when iterative decoders (such as those based on the LLR-SPA, the MSA, and the NMSA, considered in Sections IV and V) are given an input that is significantly distant from any codeword, they are expected to be unable to converge to a codeword and thus return a decoding failure.

IV. PERFORMANCE ANALYSIS IN THE STANDARD CASE

In this section we delve into the analysis of the performance of the communication system in Fig. 2, considering the parameters assumed in [1].

According to Section III, the TC rejection probability results from three contributions. Following the CCSDS recommendations, when LDPC coding is employed, the

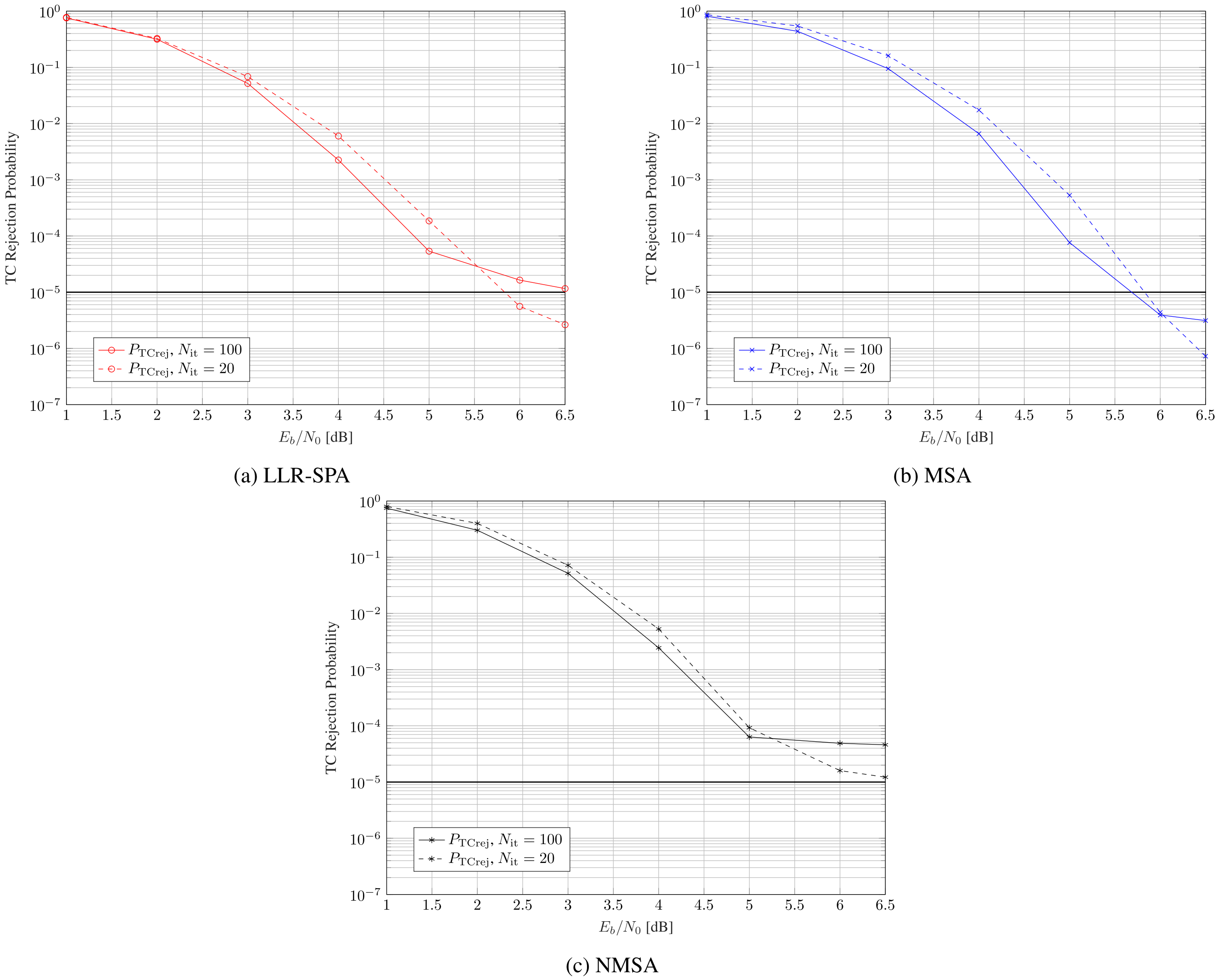

(a) LLR-SPA

(b) MSA

(c) NMSA

FIGURE 5. TC rejection probability for the three considered decoders (standard case).

start sequence consists of the following 64-bit pattern: 0347 76C7 2728 95B0 (in hexadecimal); the TS is instead formed by the following 128-bit pattern (in hexadecimal):

$$\mathbf{t} = 5555\,5556\,\mathrm{AAAA}\,\mathrm{AAAA}\,5555\,5555\,5555\,5555.$$

For the sake of results' reproducibility, we remind that the considered randomizer exploits a Linear-Feedback Shift-Register (LFSR) characterized by the polynomial $x^8 + x^6 + x^4 + x^3 + x^2 + x + 1$, which generates a pseudo-random sequence of period 255 that is summed modulo 2 to the input. When de-randomizing, the same operations of the randomization phase are applied. The standard recommends resetting the LFSR before randomizing or de-randomizing each input 128-bit sequence. Consequently, the exact randomizing (or de-randomizing) sequence XOR-ed with the codewords and the TS is always the same and is known; it is determined by the first 128 bits generated by the above LFSR.

At first, we assume that the CLTU only contains one codeword, i.e., $N = 1$. This assumption is extreme and optimistic, since P_{LDPC} gets larger for increasing values of N, according to (3). In fact, for any integer $N > 1$

$$\mathrm{CER} < 1 - (1 - \mathrm{CER})^N, \tag{7}$$

being $0 \leq \mathrm{CER} \leq 1$. Therefore, the curves we obtain in the rest of this section represent a lower bound on the actual TC rejection probability. Later, in Section VI, we will consider larger and more practical values of N.

As mentioned in the Introduction, we consider three decoding algorithms that are commonly used for decoding of CCSDS-compliant LDPC codes: the LLR-SPA, the MSA, and the NMSA with normalization factor equal to 0.8. For all these algorithms, we consider the scenarios in which the decoder runs at most $N_{\mathrm{it}} = 100$ or $N_{\mathrm{it}} = 20$ decoding iterations. We have performed Monte Carlo simulations for both the case of noisy codewords and noisy TS at the input of the decoder, stopping the simulations upon encountering

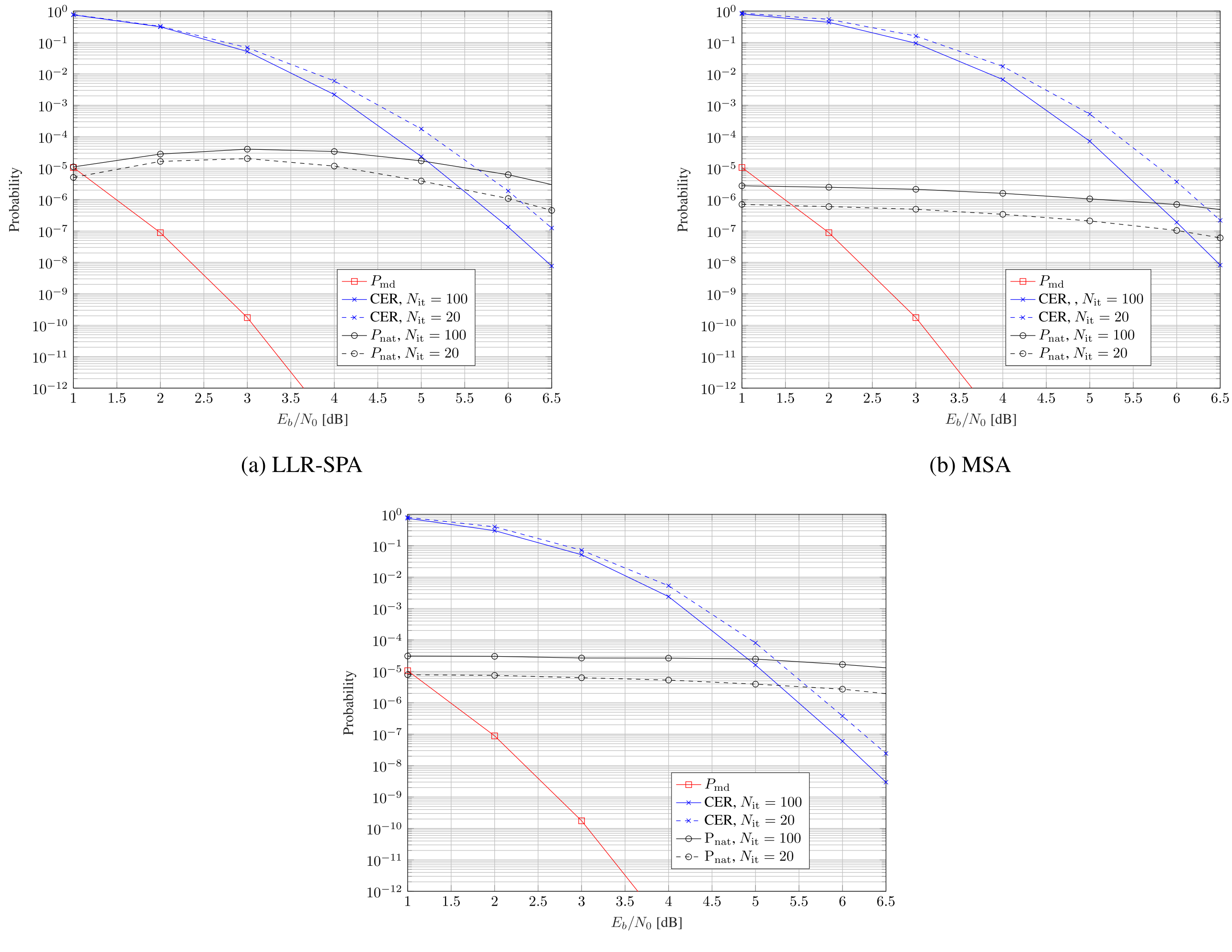

(a) LLR-SPA

(b) MSA

(c) NMSA

FIGURE 6. **Comparison of TC rejection probability's leading components for different algorithms using the newly proposed solution.**

100 decoding errors (when decoding encoded data) and 100 decoding successes (when decoding the TS).

Let us start from the missed detection probability. In Fig. 3 we show the behavior of (2), as a function of the signal-to-noise ratio per bit, computed for $S = 64$ and many different values of E. If "soft" detection approaches were employed, we could expect even lower missed detection probabilities (see [14, Fig. 5]). As we will demonstrate in the following, when E and E_b/N_0 are sufficiently large, say greater than 8 and 1.5 dB, respectively, the impact of P_{md} on P_{TCrej} becomes negligible, as it is much smaller than that of P_{LDPC} and P_{nat}. For reference, here and in the rest of the paper, we will use $E = 13$, yielding the same results as in [14, Fig. 5], for the hard-correlated case.

The results of the Monte Carlo simulations for P_{LDPC} and P_{nat} are shown in Figs. 4a, 4b, and 4c, for the standard case. For better readability, the results are grouped on the basis of the decoder. As anticipated, it is noticeable that P_{md} is always much smaller than the other leading components and does not play a significant role. Additionally, the probability of not-acknowledged termination varies very slowly with increasing values of E_b/N_0.

Combining these probabilities for the randomized TS at the receiving end to determine the TC rejection probability (1), we obtain the particularly relevant results shown in Fig. 5. We observe that the curves exhibit two different behaviors: in the leftmost part, P_{TCrej} is mainly influenced by the CER, thus assuming the typical shape of the error probability of a coded system; in the rightmost part, we notice the presence of an error floor, due to the "flatness" of P_{nat} which, for high values of $\frac{E_b}{N_0}$, becomes the dominant term.

Let us consider an hypothetical system requirement of $P_{\mathrm{TCrej}} = 10^{-5}$ around the Signal-to-Noise Ratio (SNR) working point, say about 6 dB. From Fig. 5 we notice that, if the decoder runs at most 100 iterations, only the MSA (and barely the LLR-SPA) achieves the hypothetical target performance, with relatively little margin. This is due to the fact that, in the considered E_b/N_0 range, P_{nat} is basically flat and, in particular for the LLR-SPA and NMSA decoders, it assumes relatively high values, with respect to P_{md} and

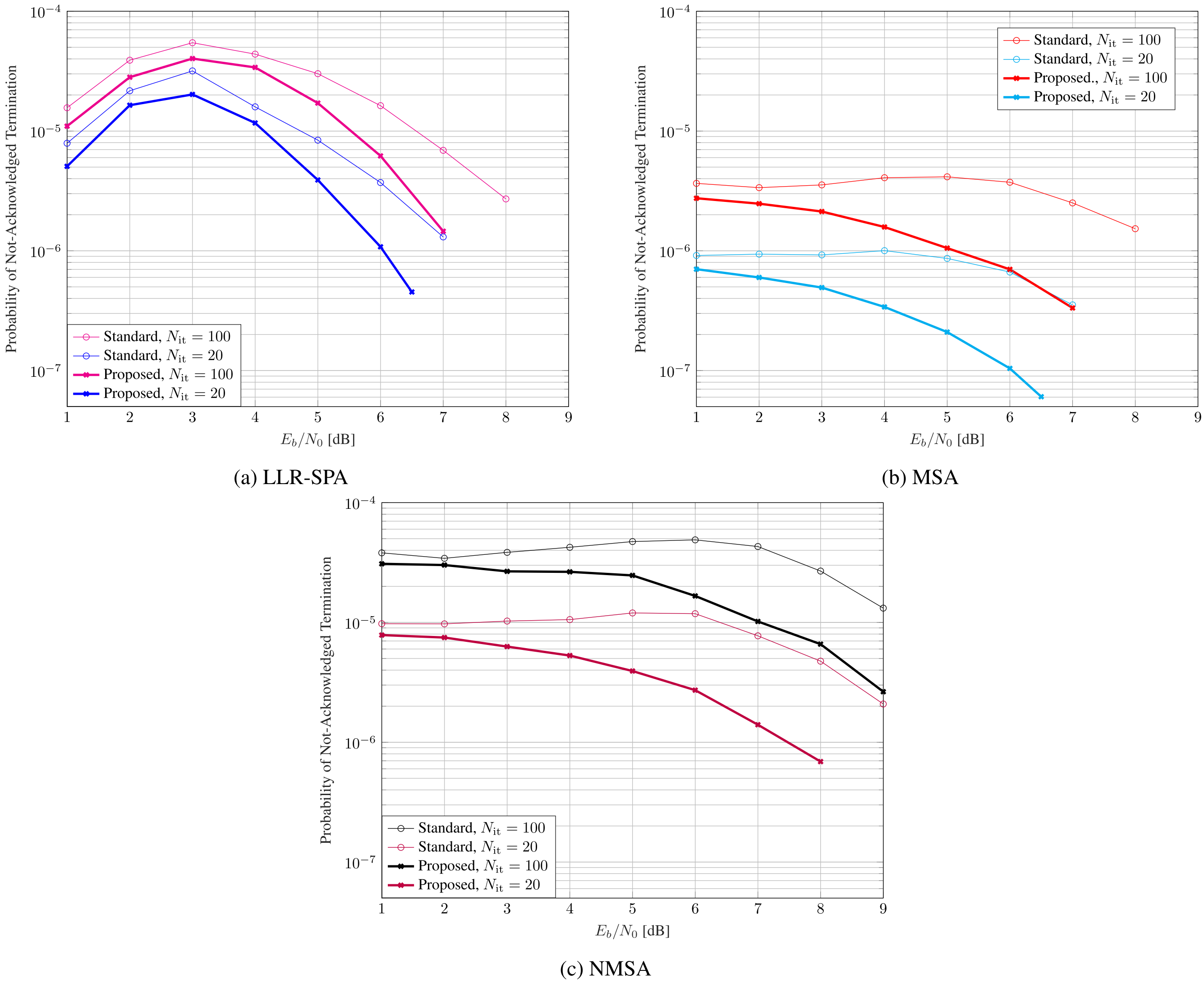

FIGURE 7. Not-acknowledged rejection probabilities for different decoding algorithms, in the standard scenario and with the newly proposed solution.

CER. Reducing the maximum number of decoding iterations improves the performance in the error floor region, at least for the case of $N = 1$ we are referring to. This happens because, by reducing N_{it}, P_{nat} (leading term in (1) when E_b/N_0 is relatively high) gets significantly smaller. In fact, when the decoder is allowed to perform a smaller maximum number of iterations, its correction capability decreases and the noisy TS is less likely to be corrected into a codeword. When P_{LDPC} is the dominant term (at relatively low values of E_b/N_0), increasing N_{it} proves beneficial, as additional iterations reduce the likelihood of decoding errors. As we show in Section VI, when N increases, P_{LDPC} might become the leading term even for relatively high values of E_b/N_0, thus canceling the beneficial effect of reducing the maximum number of decoding iterations. In the next section, instead, we propose a different solution, which always improves the overall system performance.

V. PERFORMANCE ANALYSIS WITH THE PROPOSED SOLUTION

In this section we propose a solution to improve performance, and provide many numerical results to support our conclusions.

A. TC REJECTION PROBABILITY WITH THE PROPOSED SOLUTION

In order to improve the performance discussed in Section IV, we propose to randomize the TS with the same randomizer used for the infowords, before appending it to the data in the CLTU encapsulation phase, obtaining (in hexadecimal)

$$\mathbf{t}' = \text{AA6C CB0C C243 AC5F 39DC 7AF4 640B 5D95}. \tag{8}$$

This way, at the receiving end, it gets de-randomized. The component probabilities (at the receiving end) in this novel

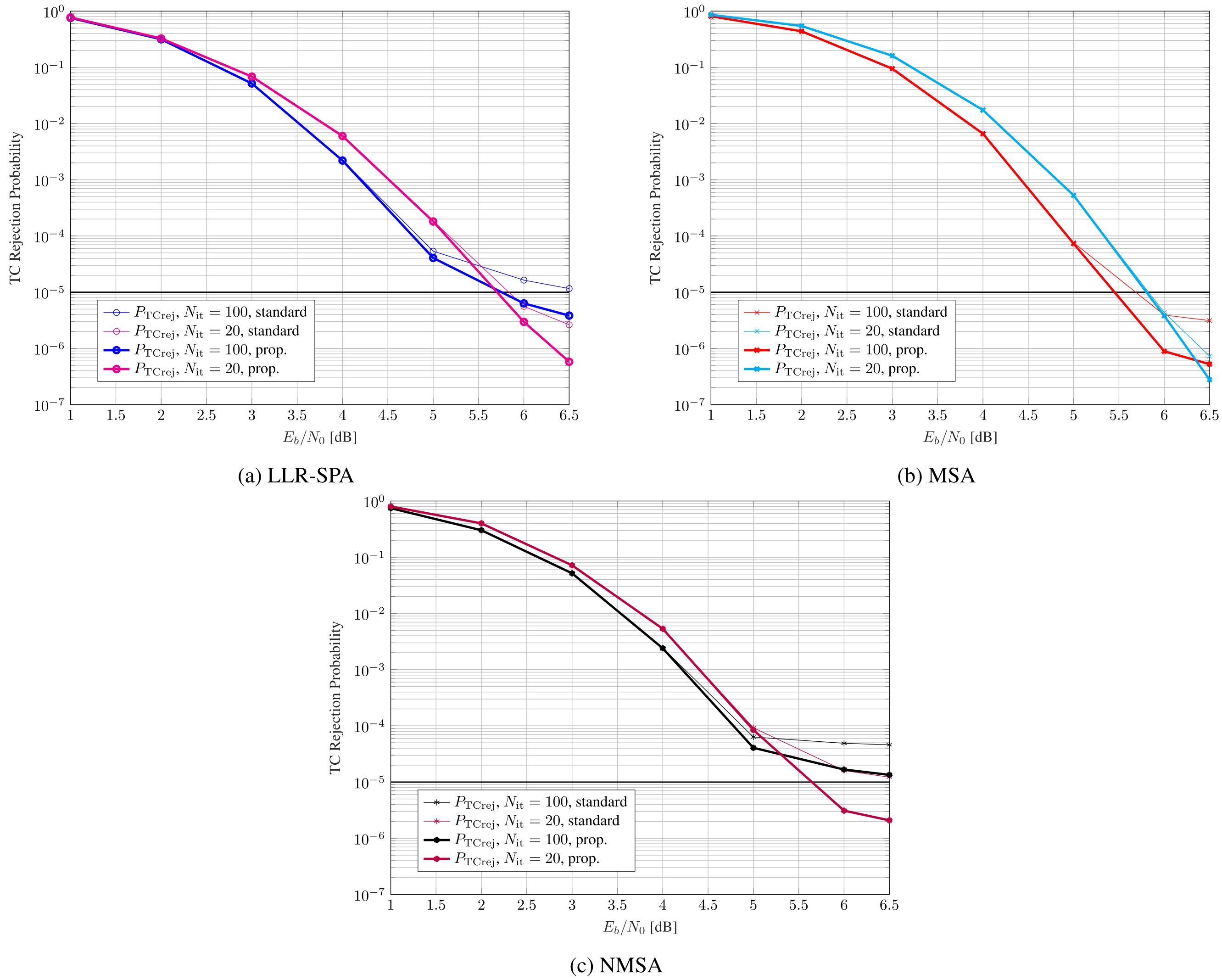

FIGURE 8. Comparison of TC rejection probabilities using different decoders for both the standard solution and the newly proposed solution.

case are shown in Figs. 6a, 6b, and 6c for the LLR-SPA, the MSA, and the NMSA, respectively. We observe that P_{nat} is much smaller in all these cases, with respect to the standard case. A more thorough comparison of the P_{nat} behaviors is illustrated in Fig. 7, which is particularly relevant in highlighting the significance and the usefulness of our proposal. For the sake of evidence, the curves associated to the proposed solution are thicker. It is remarkable that when the decoder processes the noisy (and randomized) TS we propose instead of the standard one, independently of the chosen algorithm, P_{nat} is always dramatically smaller than the corresponding probability in the standard case, for all the considered values of E_b/N_0. It is also noticeable that, in some cases, the probability of not-acknowledged termination increases with higher values of E_b/N_0. Although this may seem counterintuitive, it is important to remember that we are not transmitting a codeword. Therefore, it is possible that higher levels of noise, when added to the TS, may on average move the received signal closer to the nearest codewords, with respect to lower levels of noise, this way increasing P_{nat}. Some further insights on this issue are provided in Appendix B.

The role of the maximum number of decoding iterations also deserves attention. When evaluating the CER, increasing the maximum number of iterations allowed, N_{it}, improves performance, as expected. However, as illustrated in Fig. 7, the not-acknowledged termination probability deteriorates with higher values of N_{it}. Although this may seem counterintuitive, the explanation lies in the dual role of the decoder. Beyond its conventional function of retrieving information from corrupted data, in the considered setting the decoder is also used for detecting the TS. When the TS is input, the goal is for the decoder to fail, thereby halting the processing of the current CLTU. A higher number of iterations increases the probability that the decoder will converge to a codeword, thus deteriorating the TS detection performance. Therefore,

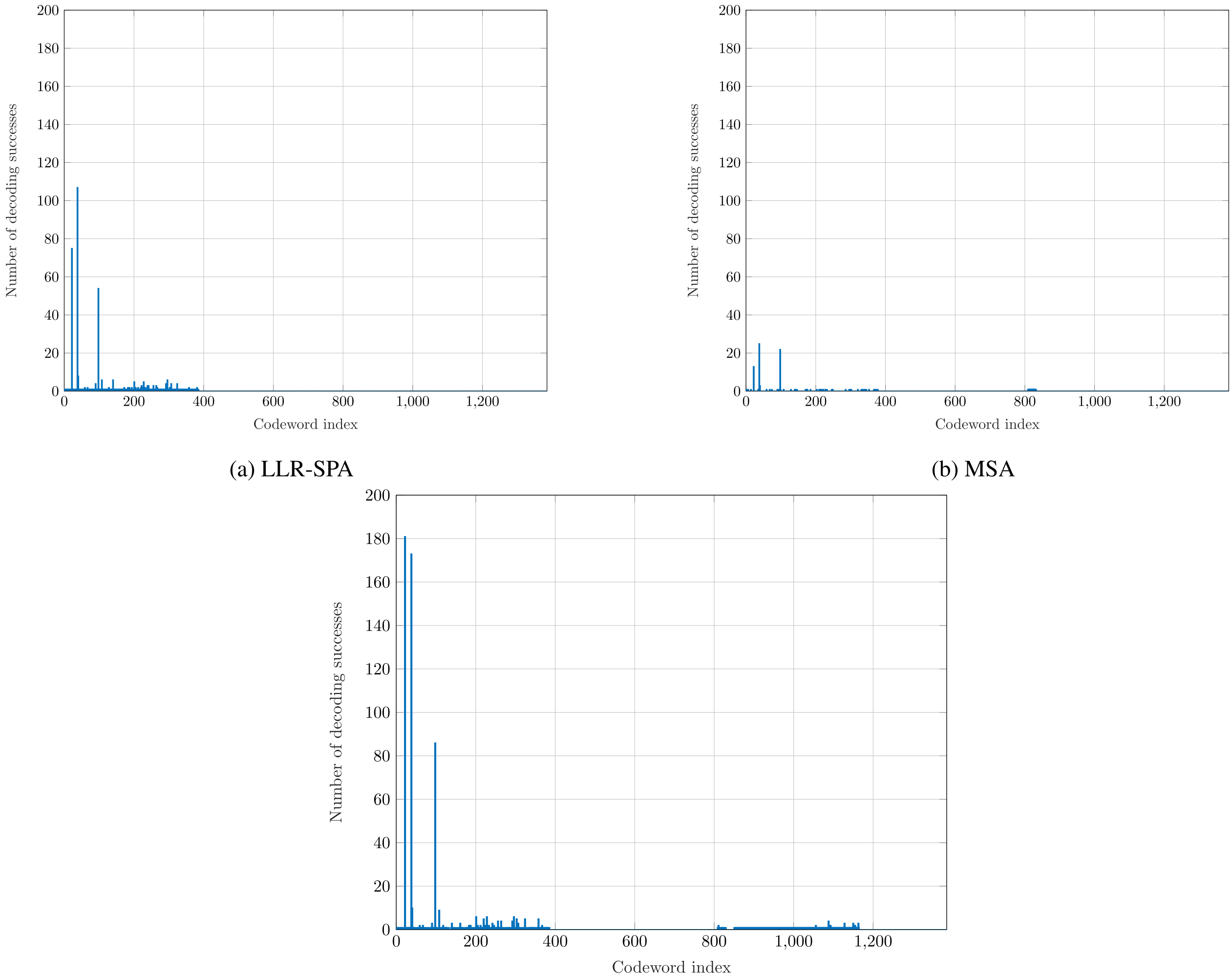

(a) LLR-SPA (b) MSA

(c) NMSA

FIGURE 9. Analysis of decoding successes of noisy TS for different decoding algorithms in the standard case.

increasing N_{it} improves the error rate performance but degrades the probability of not-acknowledged termination.

The overall TC rejection probability is shown in Fig. 8, where we also report the result obtained in the standard case. We observe that the performance in the newly proposed case is always better than that in the standard one, for all the considered decoders and maximum number of decoding iterations. Moreover, this happens not only around the considered working point, but for all values of E_b/N_0. This is an obvious consequence of the results in Fig. 7, since the probability of missed detection of the start sequence and P_{LDPC} do not change, if the TSs change. We remark that the considered target performance is reached in all cases around the working point, except for the NMSA-based decoder running 100 iterations.

It is also remarkable that, in both the standard case and the proposed one, the performance shows an error floor, especially when the maximum number of decoding iterations is set to 100, and when either the LLR-SPA or the NMSA are employed. As apparent from Figs. 4 and 6, where we show the single leading components of P_{TCrej}, the error floor is always due to the not-acknowledged termination probability P_{nat} since, for relatively large values of E_b/N_0, the values of P_{md} and CER decrease quite rapidly with E_b/N_0, and thus have a negligible impact in (1).

Another important result is that the MSA yields the best performance in terms of TC rejection probability, at least when $N = 1$. This might seem counterintuitive, since it is well-known that the MSA suffers from a performance loss in conventional error-correction applications, i.e., when the considered metric is the error rate performance. However, we need to consider that P_{TCrej} does not only depend on the CER, but also on the missed detection probability and on the not-acknowledged probability. The missed detection probability does not depend on the employed decoder. The not-acknowledged probability, instead, decreases when the TS is not identified as a codeword. In other words, the more failures the decoder produces when processing the noisy TS,

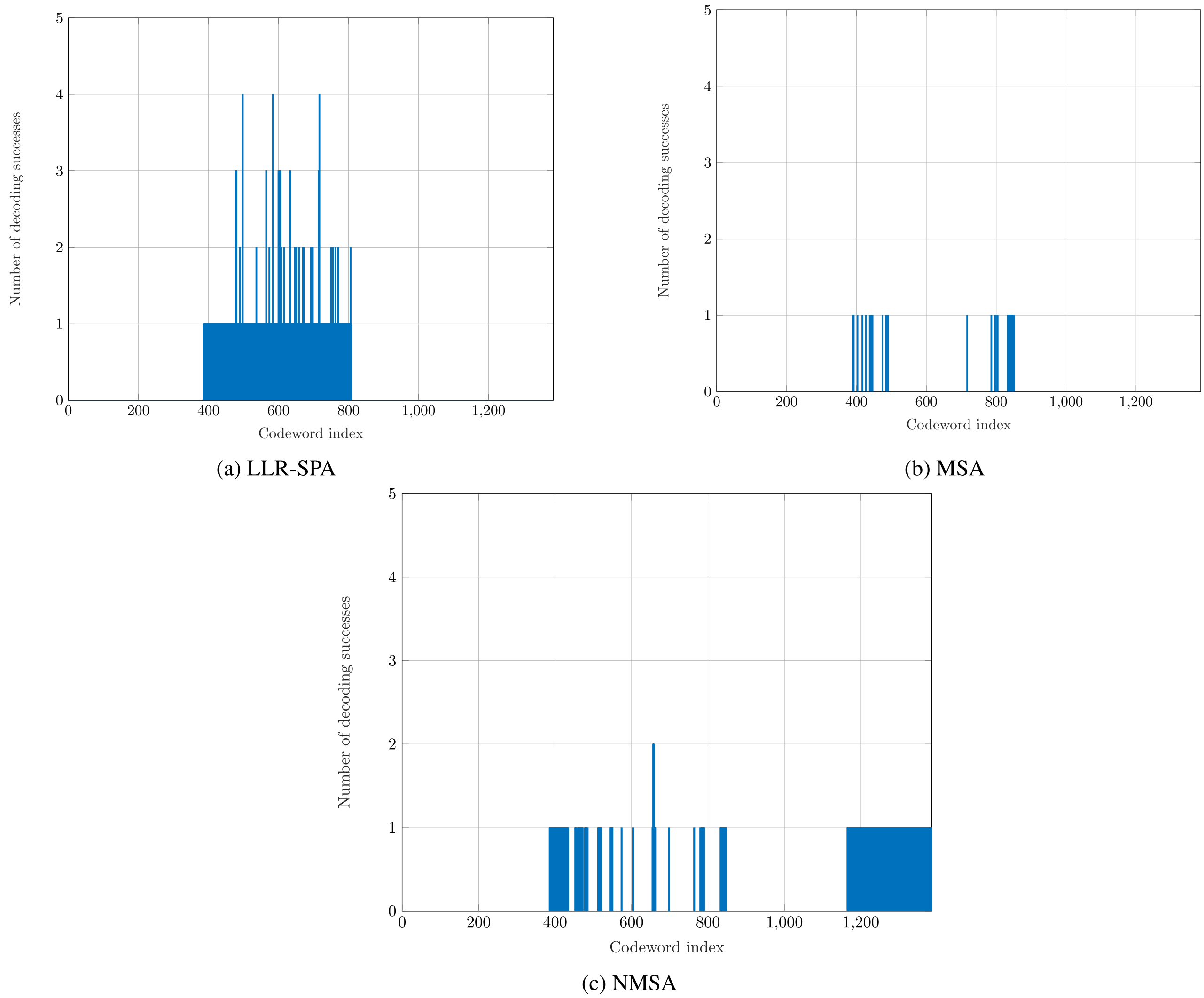

FIGURE 10. Analysis of decoding successes of noisy TS for different algorithms when applying the newly proposed solution.

the lower the not-acknowledged probability (and, thus, the lower the TC rejection probability). Therefore, we are dealing with a trade-off, since on the one hand we want a powerful decoder which is able to correctly decode codewords even when they are very noisy (in order to get a low CER), but on the other hand we want a decoder which does not decode the TS, associating it to a codeword. Our numerical results show that, in the considered setting, the MSA leads to the best overall performance.

B. DECODER CONVERGENCE ANALYSIS ON THE NOISY TS

Since the results presented in the previous subsection are worse for the standard case than for the proposed one, let us analyze the rate at which the considered decoders converge to a codeword when fed with the noisy TS, running 100 decoding iterations. The latter choice is motivated by the fact that, since the probability of not-acknowledged termination is larger than for 20 decoding iterations, we expect to get a larger decoder convergence rate. For such a purpose, we count the number of times the decoder converges to a generic codeword, starting from the noisy TS, by considering 3 000 000 decoding instances,[2] which ensures a good statistical confidence. The codewords the decoder converges to are univocally identified by a codeword index in the figures, ranging between 1 and 1 384. The simulated values of E_b/N_0 range from 0 to 7 dB, with a step of 1 dB, and the shown numbers collect the decoding successes for the whole range of E_b/N_0 we have considered. This choice follows from the fact that we are interested in studying the anomalous behaviors independently of the value of the signal-to-noise ratio. On the other hand, in Appendix B we will separate the events and we will show the number of decoding

[2]In this case, we run a fixed number of transmissions, rather than transmitting until encountering a fixed number of decoding successes (as done, for example, in Sections IV and V-A). As shown in Appendix B, this allows a fair comparison of the decoding success rate for different values of E_b/N_0.

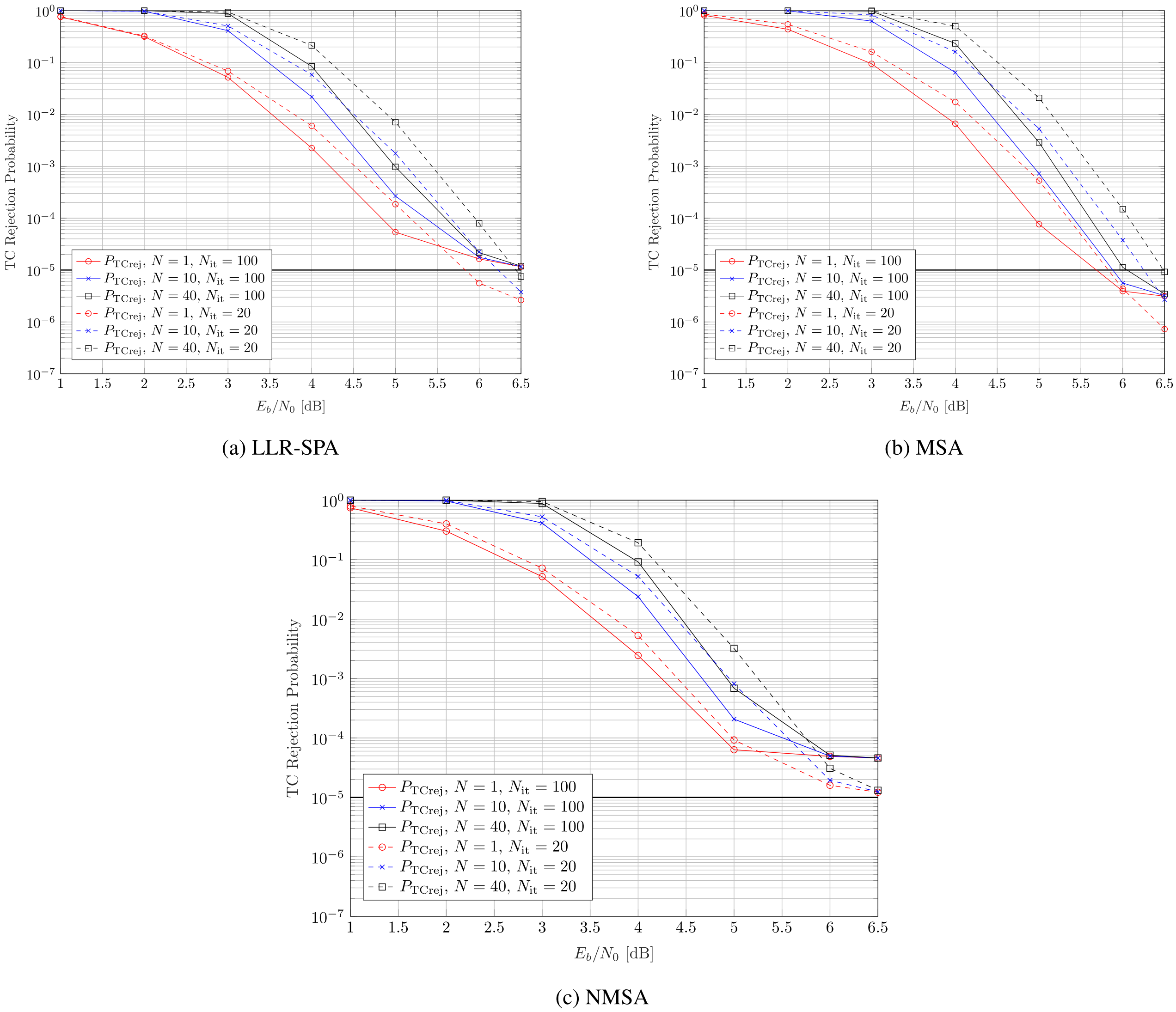

FIGURE 11. **TC rejection probability using different decoders and CLTU lengths in the standard case.**

successes, having TS in input, as a function of the signal-to-noise ratio.

Observing Figs. 9a, 9b, and 9c, obtained with the three different decoders, it is evident that each decoder very frequently converged from the noisy TS to one of three codewords, identified by the codeword indexes 22, 38, and 98 (each codeword index naturally corresponds to a distinct codeword, in the order they were produced by the decoder). We have verified that the Hamming distance between the TS and these codewords is 15. Explicitly, these codewords are (in hexadecimal):

- AE6C EF4C C057 BC7F 1DDC FBF4 641B 5D85
- AAEC 8F0C CA43 2C5F 3F58 78F4 048B 1DB5
- 0A4C 8B0C C34B ACDD 29DD FEF4 250B 5D97

Then, we can say that, given the TS as input, the LLR-SPA, MSA, and NMSA decoders frequently converge towards the aforementioned three codewords, since they are at a relatively low minimum Hamming distance from the TS itself. The specific number of decoding successes justify the fact that the MSA-based decoder has the best performance in terms of probability of not-acknowledged termination, followed by the LLR-SPA-based decoder, and then by the NMSA-based decoder (see Fig. 7).

Simulation has been repeated by adopting the newly proposed TS and results are reported in Fig. 10. We observe that the peaks that were observed in Fig. 9 practically disappear when the solution we propose is adopted. Most importantly, the three histograms for the de-randomized case clearly show that the codewords are mistaken for the TS significantly fewer times, indicating that they are sufficiently and almost evenly distant from the de-randomized TS. In particular, the Hamming distance of the TS to the closest misunderstood codewords is 18, rather than 15 of the randomized case.

To ensure that no other codewords exhibit a smaller Hamming distance than 18 from the TS, we employed Stern's

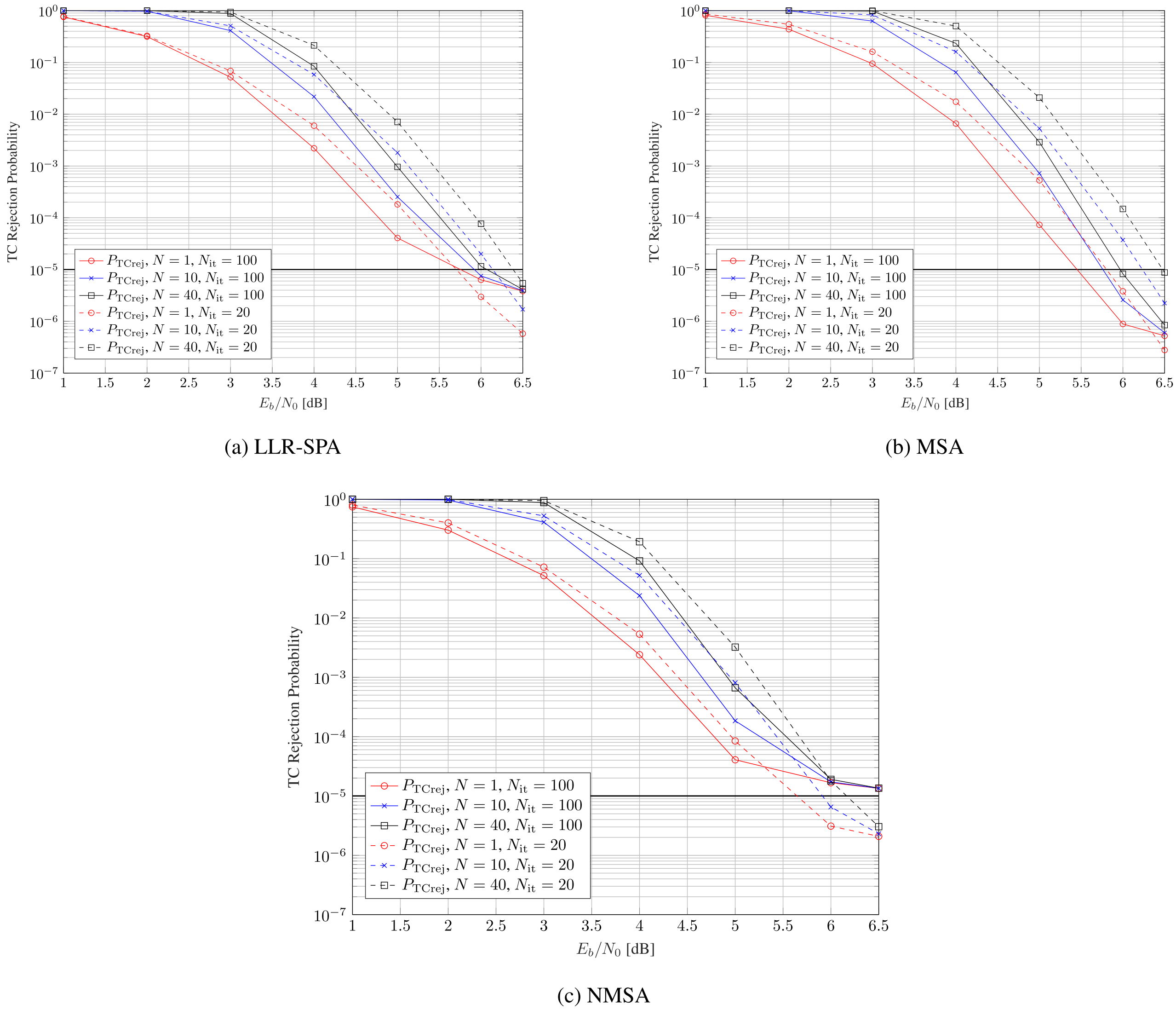

FIGURE 12. TC Rejection Probability for different decoders and CLTU lengths, when using the newly proposed TS.

information set decoding method [15] and the technique outlined in [16] to find several low-weight codewords of the (128, 64) code. Our analysis reveals that: (i) none of these codewords has a Hamming distance smaller than 18 from the TS, (ii) 73 codewords differ from the TS in 18 positions, (iii) 3 967 codewords have a Hamming distance of 20 from the TS.

VI. ANALYSIS FOR A LARGER NUMBER OF CODEWORDS IN THE CLTU

In this section we extend the analysis to the case of $N > 1$, that is, the CLTU contains more than one codeword. This reflects a more general scenario since, in space missions, data longer than one word clearly span over more codewords.

A. NUMERICAL ANALYSIS FOR A CLTU WITH MORE THAN ONE CODEWORD

As an example, we compare the performance of the system when transmitting a CLTU with encoded data consisting of a single codeword ($N = 1$) to those with encoded data consisting of $N = 10$ and $N = 40$ codewords. As expected from the discussion in Section IV, the system performance is worse in the case of a CLTU containing 10 and 40 codewords than in the case with a single codeword. This is clearly shown in Figs. 11 and 12 for the standard and the proposed solution, respectively. According to (7), such a result would also be confirmed by considering other values of $N > 1$. So, the case with $N = 1$ should be seen as the best scenario. Notice that, generalizing the analysis, we have kept the same system requirements as in Section IV.

From Figs. 11 and 12, we also observe that, when E_b/N_0 is small (say not larger than 5 dB), in both the standard case and the newly proposed one, decreasing the number of iterations does not yield any advantage in terms of TC rejection probability, independently of N. This perfectly aligns with previous Fig. 8 (characterized by $N = 1$), where the reduction of the maximum number of iterations also leads to a reduction in the TC rejection probability when E_b/N_0 is larger than

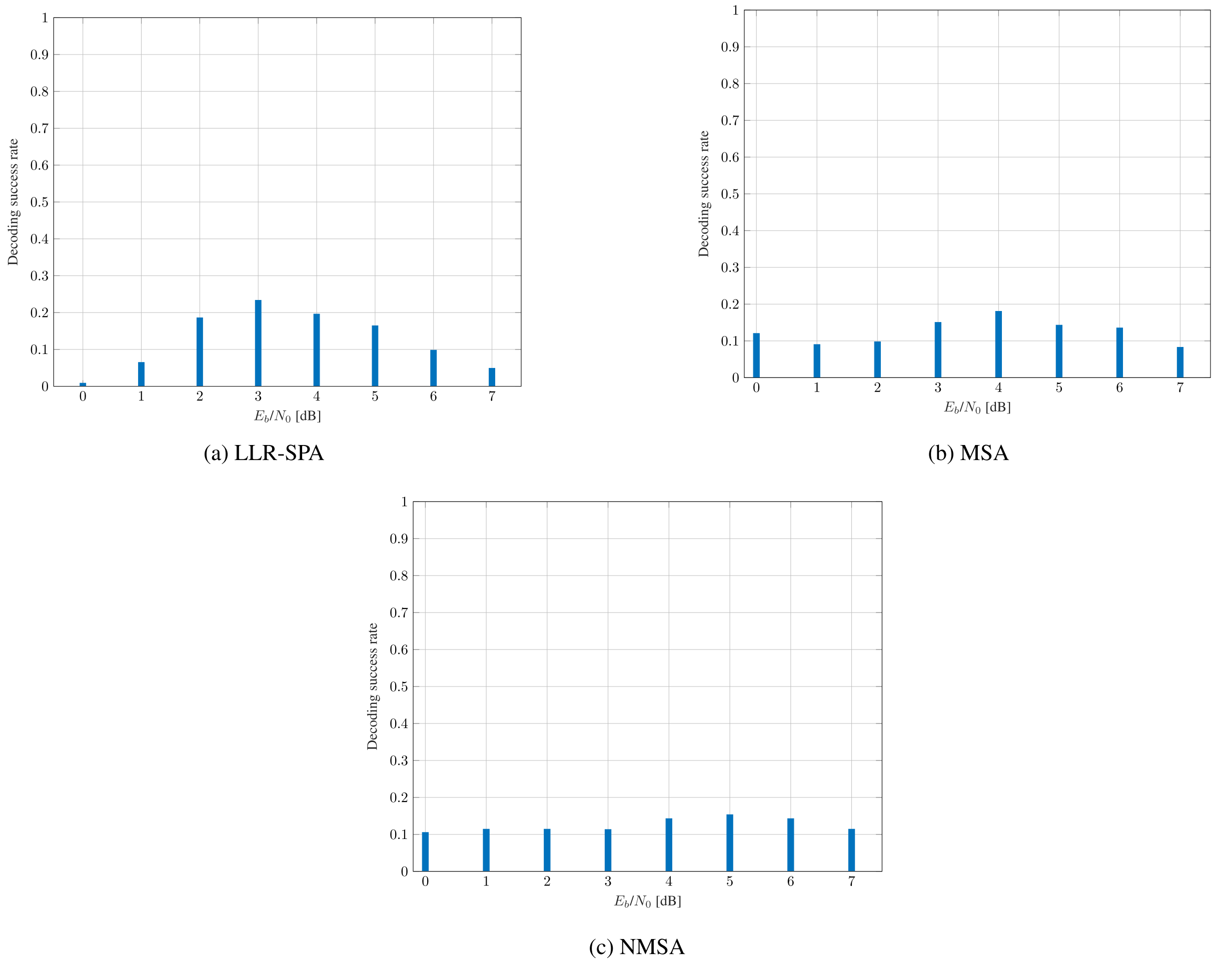

FIGURE 13. Decoding success rate for different E_b/N_0 values in the standard case.

5 dB. However, in the (relatively) large E_b/N_0 regime, this might not happen when $N = 10$ or $N = 40$ (corresponding to the blue and black curves in Figs. 11 and 12, respectively). For example, when employing the MSA-based decoder, with $N = 10$ or $N = 40$, decreasing the maximum number of iterations from 100 to 20 does not yield any advantage for any of the considered values of E_b/N_0, especially when $N = 10$. On the contrary, when the NMSA-based decoder is used, for relatively high values of E_b/N_0, the system performance benefits from the reduction of the maximum number of decoding iterations. This is a consequence of the fact that the NMSA is the decoding algorithm with the smallest CER. Therefore, since N and E_b/N_0 are both not very large, the leading term in (1) remains the not-acknowledged termination probability P_{nat}.

Generally, Figs. 11 and 12 show that, depending on the considered decoder, the operating point and the CLTU length, and assuming the TS is employed and detected using a decoder, it may be necessary to optimize the number of iterations used. It is indeed evident that increasing the maximum number of iterations reduces the CER but increases the P_{nat}, as the additional iterations aid decoder convergence. In other words, the increase of the maximum number of iterations is beneficial for coded data, since it helps the decoder to converge more often to a codeword, but undesirable for the TS, which should instead trigger a decoding error. Therefore, finding the optimal trade-off might be crucial.

Table 1 summarizes the TC rejection probabilities (P_{TCrej}) at $E_b/N_0 = 6$ dB for different decoding schemes and configurations. Results are reported for different values of the maximum number of iterations (N_{it}), the number of codewords in the CLTU (N), and the type of TS (Standard or Proposed). The probabilities are provided for the three considered decoding algorithms: LLR-SPA, MSA, and NMSA. This comparison highlights the superiority of the proposed solution with respect to the standard one.

B. REMARKS ON LARGE VALUES OF THE SIGNAL-TO-NOISE RATIO

Running Monte Carlo simulations to estimate CER values on the order of 10^{-8} or lower is computationally demanding. For the considered (128, 64) LDPC code, this significantly hinders numerical analysis for E_b/N_0 values of 7 dB or higher. However, assuming that the CER continues to drop faster than P_{nat} for values slightly greater than 7 dB, we can

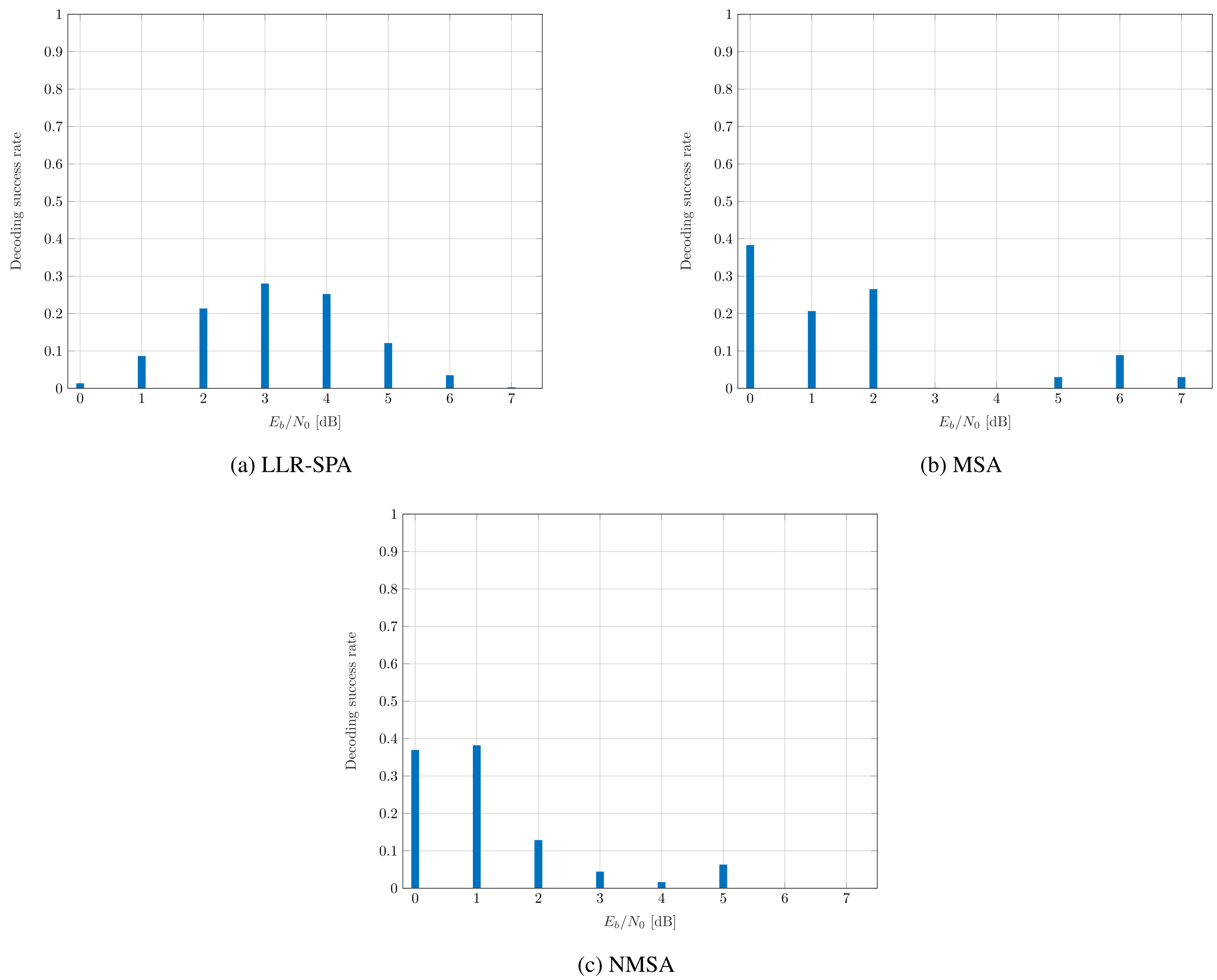

FIGURE 14. Decoding success rate for different E_b/N_0 values when the newly proposed solution is adopted.

TABLE 1. Comparison of P_{TCrej} for $E_b/N_0 = 6$ dB.

N_{it}	N	TS	P_{TCrej}		
			LLR-SPA	MSA	NMSA
100	1	Stand.	1.64×10^{-5}	3.92×10^{-6}	4.90×10^{-5}
		Prop.	6.33×10^{-6}	8.89×10^{-7}	1.67×10^{-5}
	10	Stand.	1.76×10^{-5}	5.63×10^{-6}	4.95×10^{-5}
		Prop.	7.54×10^{-6}	2.59×10^{-6}	1.72×10^{-5}
	40	Stand.	2.16×10^{-5}	1.13×10^{-5}	5.13×10^{-5}
		Prop.	1.16×10^{-5}	8.26×10^{-6}	1.90×10^{-5}
20	1	Stand.	5.60×10^{-6}	4.36×10^{-6}	1.60×10^{-5}
		Prop.	2.97×10^{-6}	3.80×10^{-6}	3.10×10^{-6}
	10	Stand.	2.26×10^{-5}	3.77×10^{-5}	1.94×10^{-5}
		Prop.	2.00×10^{-5}	3.71×10^{-5}	6.52×10^{-6}
	40	Stand.	7.93×10^{-5}	1.49×10^{-4}	3.08×10^{-5}
		Prop.	7.67×10^{-5}	1.48×10^{-4}	1.79×10^{-5}

leverage the insights from Section III-B to infer some conclusions. In particular, according to (5), for small to moderate values of N, we can expect that the leading term in (1) is the not-acknowledged termination probability P_{nat}. In other words, we expect the trend of the TC rejection probability to be determined by P_{nat}. However, we also remark that, for extremely large values of E_b/N_0, the TS (especially when the proposed solution is adopted) always causes a decoding error, asymptotically yielding $P_{\text{nat}} \to 0$ when $E_b/N_0 \to \infty$. Therefore, clearly, if the error rate performance of the LDPC code exhibits an error floor at any point, a more comprehensive analysis will be necessary. This entails delving into the causes of the error floor, which may include investigating specific code properties and decoding algorithm limitations, such as trapping sets [17], pseudo-codewords [18], and other harmful objects [19]. This analysis goes beyond the scope of this paper and is left for future works.

VII. CONCLUSION AND FUTURE WORKS

We have analyzed the performance of a TC CCSDS-compliant communication scheme incorporating LDPC-coded transmissions in satellite systems, with a focus on the optional tail sequence that may be required for termination. We have evaluated the TC rejection probability, both theoretically and numerically, across various operation conditions, involving the length of the CLTU, the decoding algorithm and the maximum number of decoding iterations. We have demonstrated that a well-designed tail sequence, actually different from the standard one, which is sufficiently distant from any valid codeword according to a chosen metric, effectively triggers a decoding error, thereby aiding correct termination of the CLTU.

As mentioned, we have evaluated the performance using different iterative decoding algorithms, namely the LLR-SPA, the MSA, and the NMSA. Our results show that, in the considered setting, the MSA-based decoder performs better than the other two algorithms when the optional TS is employed to trigger a decoding error. Our analysis also indicates that reducing the maximum number of decoding iterations does not always provide an advantage in terms of TC rejection probability, particularly when E_b/N_0 is below 5 dB. However, for extremely short CLTUs and for moderate to high values of E_b/N_0, reducing the number of iterations can enhance performance, from the TS detection viewpoint, highlighting the importance of tailoring the decoding strategy to the specific context.

Through a combination of theoretical analysis and Monte Carlo simulations, we have provided a comprehensive understanding of the factors affecting TC rejection probability.

As a catalyst for future research, we foresee that it is possible to integrate the conventional iterative decoder with machine learning, thus obtaining a joint decoder and TS detector which should be able to classify a received vector as a codeword or as the TS. As training data, it might be possible to exploit the total log-likelihood ratios computed by the decoder in the decoding process. We also intend to explore a novel approach to the design of the TS. Specifically, we plan to focus on harmful structures that induce decoding errors, such as trapping sets, absorbing sets, and fully absorbing sets. While the current method of designing a TS that is distant from all codewords is based on the general ML decoding principle, an alternative approach is to consider the unique characteristics of iterative decoders commonly used for decoding LDPC codes. This is crucial because harmful patterns are not necessarily very distant from codewords.

APPENDIX A
(128, 64) LDPC CODE DESCRIPTION

The (128, 64) LDPC TC code has information length $k = 64$ and codewords length $n = 128$, and is specified by an $r \times n$ parity-check matrix $\mathbf{H}_{64\times 128}$, where $r = n - k$. This matrix is constructed from $M \times M$ submatrices, where $M = k/4 = n/8 = 16$, as follows:

$$\mathbf{H} = \begin{bmatrix} \mathbf{I}_M \oplus \mathbf{\Phi}^7 & \mathbf{\Phi}^2 & \mathbf{\Phi}^{14} & \mathbf{\Phi}^6 & \mathbf{0}_M & \mathbf{\Phi}^0 & \mathbf{\Phi}^{13} & \mathbf{I}_M \\ \mathbf{\Phi}^6 & \mathbf{I}_M \oplus \mathbf{\Phi}^{15} & \mathbf{\Phi}^0 & \mathbf{\Phi}^1 & \mathbf{I}_M & \mathbf{0}_M & \mathbf{\Phi}^0 & \mathbf{\Phi}^7 \\ \mathbf{\Phi}^4 & \mathbf{\Phi}^1 & \mathbf{I}_M \oplus \mathbf{\Phi}^{15} & \mathbf{\Phi}^{14} & \mathbf{\Phi}^{11} & \mathbf{I}_M & \mathbf{0}_M & \mathbf{\Phi}^3 \\ \mathbf{\Phi}^0 & \mathbf{\Phi}^1 & \mathbf{\Phi}^9 & \mathbf{I}_M \oplus \mathbf{\Phi}^{13} & \mathbf{\Phi}^{14} & \mathbf{\Phi}^1 & \mathbf{I}_M & \mathbf{0}_M \end{bmatrix},$$

where $\mathbf{I}_M$ is the $M \times M$ identity matrix, $\mathbf{\Phi}^i$ is the i-th right circular shift of $\mathbf{I}_M$, where $0 \leq i \leq M - 1$, and $\mathbf{0}_M$ is the $M \times M$ zero matrix. Finally, the $\oplus$ operator indicates modulo-2 addition.

APPENDIX B
DECODING SUCCESS RATE FOR DIFFERENT VALUES OF E_B/N_0

In this appendix, we provide further analysis to support the results presented in Fig. 7, expanding the discussion in Section V-B. In particular, we present the results in Figs. 9 and 10, in terms of decoding success rates, categorized by each considered value of E_b/N_0. Let us remind that data were collected by analyzing 3 000 000 transmissions of the (standard and newly proposed) TS, with 100 maximum decoding iterations.

From Figs. 13a and 14a we observe that most of the decoding successes (80%), causing a misinterpretation of the TS, for the LLR-SPA decoder, occur for $\frac{E_b}{N_0}$ between 2 and 6 dB, extremes included. This explains the results shown in Fig. 7a; in fact, for the mentioned values of $\frac{E_b}{N_0}$, most decoding successes occur, leading to higher values of P_{nat} compared to other $\frac{E_b}{N_0}$ values. For the other decoders, the aforementioned effect is less pronounced. In particular, most of the decoding successes for the MSA and the NMSA-based decoders occur for small values of E_b/N_0, when the newly proposed TS is adopted.

ACKNOWLEDGMENT

The authors thank Dr. Andrea Modenini for his valuable insights.

The conclusion reported in this article are the opinion of the authors and do not represent the official position of the European Space Agency.

REFERENCES

[1] *TC Synchronization and Channel Coding. Issue Recommendation for Space Data System Standard, Blue Book CCSDS 231.0-B-4*, Consultative Commitee for Space Data Syst., Washington, DC, USA, Jul. 2021.

[2] A. Modenini and B. Ripani, "A tutorial on the tracking, telemetry, and command (TT&C) for space missions," *IEEE Commun. Surveys Tuts.*, vol. 25, no. 3, pp. 1510–1542, 3rd Quart., 2023.

[3] J. Massey, "Optimum frame synchronization," *IEEE Trans. Commun.*, vol. COM-20, no. 2, pp. 115–119, Apr. 1972.

[4] M. Chiani and M. G. Martini, "On sequential frame synchronization in AWGN channels," *IEEE Trans. Commun.*, vol. 54, no. 2, pp. 339–348, Feb. 2006.

[5] S. Pfletschinger, M. Navarro, and P. Closas, "Frame synchronization for next generation uplink coding in deep space communications," in *Proc. IEEE Global Commun. Conf. (GLOBECOM)*, Dec. 2015, pp. 1–6.

[6] A. Hocquenghem, "Codes correcteurs d'erreurs," *Chiffres*, vol. 2, pp. 147–156, Sep. 1959.

[7] R. C. Bose and D. K. Ray-Chaudhuri, "On a class of error correcting binary group codes," *Inf. Control*, vol. 3, no. 1, pp. 68–79, Mar. 1960.

[8] R. G. Gallager, "Low-density parity-check codes," *IRE Trans. Inf. Theory*, vol. 8, no. 1, pp. 21–28, Jan. 1962.

[9] K. Andrews, "Tail sequence search for the (128,64) uplink LDPC code," Presented at the CCSDS Spring Meeting, 2017.

[10] X.-Y. Hu, E. Eleftheriou, D.-M. Arnold, and A. Dholakia, "Efficient implementations of the sum-product algorithm for decoding LDPC codes," in *Proc. IEEE Global Telecommun. Conf.*, vol. 2, Nov. 2001, pp. 1036–1026E.

[11] M. P. C. Fossorier, M. Mihaljevic, and H. Imai, "Reduced complexity iterative decoding of low-density parity check codes based on belief propagation," *IEEE Trans. Commun.*, vol. 47, no. 5, pp. 673–680, May 1999.

[12] J. Chen and P. Fossorier, "Density evolution for BP-based decoding algorithms of LDPC codes and their quantized versions," in *Proc. IEEE Global Telecommun. Conf. (GLOBECOM)*, vol. 2, Nov. 2002, pp. 1378–1382.

[13] *TC Synchronization and Channel Coding—Summary of Concept and Rationale. Informational Report, Green Book CCSDS 230.1-G-3*, Consultative Commitee for Space Data Syst., Washington, DC, USA, Oct. 2021.

[14] M. Baldi, M. Bertinelli, F. Chiaraluce, P. Closas, R. Garello, N. Maturo, M. Navarro, J. M. Palomo, E. Paolini, S. Pfletschinger, P. F. Silva, L. Simone, and J. Vilà-Valls, "NEXCODE: Next generation uplink coding techniques," in *Proc. Int. Workshop Tracking, Telemetry Command Syst. Space Appl. (TTC)*, Sep. 2016, pp. 1–8.

[15] J. Stern, "A method for finding codewords of small weight," in *Coding Theory and Applications* (Lecture Notes in Computer Science), vol. 388, G. D. Cohen and J. Wolfmann, Eds. New York, NY, USA: Springer, 1989, pp. 106–113.

[16] X.-Y. Hu, M. P. C. Fossorier, and E. Eleftheriou, "On the computation of the minimum distance of low-density parity-check codes," in *Proc. IEEE Int. Conf. Commun.*, vol. 2, Jun. 2004, pp. 767–771.

[17] T. Richardson, "Error floors of LDPC codes," in *Proc. 41st Annu. Allerton Conf.*, Monticello, IL, USA, Sep. 2003, pp. 1426–1435.

[18] R. Koetter and P. O. Vontobel, "Graph covers and iterative decoding of finite-length codes," in *Proc. 3rd Int. Symp. Turbo Codes Rel. Topics*, Sep. 2003, pp. 75–82.

[19] M. Battaglioni, F. Chiaraluce, M. Baldi, M. Pacenti, and D. G. M. Mitchell, "Optimizing quasi-cyclic spatially coupled LDPC codes by eliminating harmful objects," *EURASIP J. Wireless Commun. Netw.*, no. 67, Jul. 2023.

REBECCA GIULIANI (Graduate Student Member, IEEE) received the bachelor's and master's (summa cum laude) degrees in electronic engineering from the Università Politecnica delle Marche (UNIVPM), Ancona, Italy, in 2021 and 2023, respectively, where she is currently pursuing the Ph.D. degree in information engineering. Her research focuses on coded satellite communications and more in general on the communication systems' reliability and security, with particular interest on physical layer security.

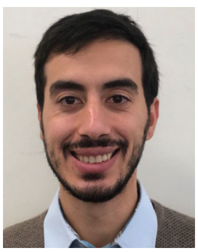

MASSIMO BATTAGLIONI (Member, IEEE) received the Laurea and Laurea Magistrale (summa cum laude) degrees in electronic engineering and the Ph.D. degree in information engineering from the Università Politecnica delle Marche (UNIVPM), Ancona, Italy, in 2013, 2015, and 2019, respectively. In 2017, he was a Visiting Student with the Electrical and Information Technology Department, LTH, Lund University, Sweden. In 2018, he was a Visiting Student with the Klipsch School of Electrical and Computer Engineering, New Mexico State University (NMSU), Las Cruces, NM, USA; and the School of Electrical and Electronic Engineering, University College Dublin, Ireland. Since 2024, he has been a tenure-track Researcher with the Department of Information Engineering, UNIVPM. His research interests include coding techniques for communications reliability, with particular attention to LDPC codes and their application to cryptography and blockchain. He is also interested in cyber risk assessment methods. He serves as an Editor for IEEE Communications Letters.

MARCO BALDI (Senior Member, IEEE) received the Laurea degree (Hons.) in electronics engineering and the Ph.D. degree in electronics, computer, and telecommunications engineering from the Università Politecnica delle Marche (UNIVPM), Ancona, Italy. Since 2019, he has been an Associate Professor with the Department of Information Engineering, UNIVPM, where he also coordinates the local node of the CINI Cybersecurity National Laboratory and takes part in the Research and Service Center for Privacy and Cybersecurity (CRiSPY). He has co-authored more than 200 scientific articles and one book, and holds four patents. His research interests include coding and cryptography for information security and reliability. He is a member of AEIT, CINI, CNIT, IEEE Communications Society, and IEEE Information Theory Society. He serves as an Area Editor in coding for IEEE Communications Letters and an Associate Editor for the *EURASIP Journal on Wireless Communications and Networking*.

FRANCO CHIARALUCE (Senior Member, IEEE) received the Laurea degree (summa cum laude) in electronic engineering from the University of Ancona, in 1985. Since 1987, he has been with the Department of Electronics and Automatics, University of Ancona. He is currently a Full Professor in telecommunications with the Università Politecnica delle Marche (UNIVPM), Ancona, Italy, where he is also the Director of the Department of Information Engineering (DII). He has co-authored more than 300 scientific articles and three books and holds three patents. On his research topics, he collaborates with national and international companies. His main research interests include various aspects of communication systems theory and design, with a special emphasis on error-correcting codes, cryptography, and physical layer security. He is a member of IEICE.

NICOLA MATURO (Member, IEEE) received the M.S. degree in electronic engineering (cum laude) and the Ph.D. degree in telecommunication engineering from the Università Politecnica delle Marche, Ancona, Italy, in 2012 and 2015, respectively. From January 2016 to July 2017, he was a Postdoctoral Researcher with the Department of Information Engineering, Università Politecnica delle Marche, where he worked on error correcting coding techniques under some ESA research projects. From August 2017 to July 2021, he was a Research Scientist with the Interdisciplinary Centre for Security, Reliability and Trust, University of Luxembourg, mainly working in the satellite communication domain. From August 2021 to November 2023, he was part of HE Space, as a TT&C Engineer with the TEC-EST Section, European Space Agency (ESA)-ESTEC, and in December 2023, he became a full time Employee of ESA. He is a member of the CCSDS Coding and Synchronization Working Group, since 2015.